

Quark cluster signatures in deuteron electromagnetic interactions

C.E. Carlson

Physics Department, College of William and Mary, Williamsburg, Virginia 23187

K.E. Lassila

Department of Physics and Astronomy, Iowa State University, Ames, Iowa 50011

(Received 12 January 1994)

A suggestion is made for distinguishing $2N$ and $6q$ short-range correlations within the deuteron. The suggestion depends upon observing high momentum backward nucleons emerging from inelastic electromagnetic scattering from a deuteron target. A simple model is worked out to see the size of effects that may be expected.

PACS number(s): 24.85.+p, 12.39.Mk, 13.85.Ni, 25.30.Rw

I. INTRODUCTION

When the constituents of a nucleus are far apart, a description in terms of neutrons and protons is accurate. The question is what happens to the material inside the nucleons when the pieces come close to each other. We shall consider a way to help resolve this issue using electromagnetic scattering from a deuteron. In particular, we shall be interested in semexclusive measurements where a backward (relative to the incoming photon) high momentum nucleon emerges from the reaction.

One view of what happens when the nucleons come close to each other is that they never do. A repulsive force keeps them apart. One may additionally suppose that even if the nucleons are pushed close together they maintain their nucleonic character and behave as recognizable neutrons and protons. This viewpoint we shall refer to as the two-nucleon, or $2N$, model for the behavior of nuclear material at short interparticle distances. (Note that it is not possible to take a neutron—three quarks in an S state with the correct spin, isospin, and color—and precisely overlap it with a proton. The Pauli principle at the quark level prevents it.)

An alternative viewpoint is that if two nucleons come sufficiently close together, the quarks within them reorganize or mix into a new state where each quark is in the lowest energy spatial state, and the color-spin-flavor part of the quark wave function is uniquely fixed by the requirement that it be a totally antisymmetric colorless state of the desired spin and isospin [1]. The six quarks may thus lie top of each other. This quark cluster model is also an extreme viewpoint, and we refer to it as a six-quark or $6q$ model.

In neither the $2N$ model nor the $6q$ model do we believe that the backward nucleon comes from the nucleon or the quark that was struck [2]. Rather, the backward nucleons come from debris that remains after the item that was struck is driven strongly forward. For example, to describe backward proton production in the $2N$ model, it must be the neutron that is struck, breaking up the bound state, with the proton emerging with the Fermi momentum it had at the moment of breakup. The high momentum of the backward nucleon is a tag ensur-

ing we are seeing a strongly correlated system that has the highest probability of being an unusual configuration. We shall show that there are features of backward nucleon production that are characteristically different for $2N$ and $6q$ models and allow us to adjudicate between them. We have previously commented [3, 4] upon using neutrino production of backward protons [5–8] to similar ends.

In the $6q$ model, emitting a backward proton begins with one quark being struck and driven forward. The proton is formed out of the remaining five quarks, plus possible higher Fock components, and we refer to the process of forming hadrons as the “fragmentation” of the five-quark residuum. This terminology follows common usage for the production of hadrons from any color nonsinglet QCD object, quark and gluon jets being the most familiar. In the present case, we persist with the “fragmentation” nomenclature even though recombination may be the process chiefly at work. In any case, the $6q$ model can produce a backward proton spectrum which agrees with data from neutrino reactions, for backward hemisphere proton momentum above about 300 MeV [3]. However, so can the $2N$ model, with enhanced high momentum components [9]. To distinguish the models, we need indicators that are independent of quantities that are unknown or implementation sensitive, and which give predicted results which are distinct for the $2N$ and $6q$ models. For weak interactions, cross section ratios for neutrino and antineutrino initiated backward proton production are a suitable choice [4]. Similar opportunities exist for electromagnetic interactions.

A suggestion for a ratio to examine in the electromagnetic case, particularly at fixed backward proton momentum and varying Bjorken x , is given in Sec. II, along with some numerical estimates of the differences between the two models. Section III contains a series of comments, starting with some remarks about when and if one might expect a $6q$ configuration to dominate, and related matters, and continuing with comments on electron energy needs and possibilities at various (existing or proposed) accelerators or facilities, including CEBAF, ELFE, Hermes, LEP, and Fermilab. Also remarked upon in Sec. III is an observation regarding decreases in average Bjorken

x with increases in backward nucleon momentum, which was originally made in the context of the $2N$ model, but is an example of something that should be reasonably true for most any model. We conclude in Sec. IV.

II. SIGNATURES OF SHORT DISTANCE CORRELATIONS

A. General

The cross section for inelastic electromagnetic scattering of a lepton from a stationary target is (in the scaling region and neglecting σ_L/σ_T)

$$\frac{d\sigma}{dx dy} = \frac{4\pi \alpha_{\text{em}}^2 m_N E}{Q^4} \left[1 + (1-y)^2 \right] F_2(x, Q^2), \quad (1)$$

where E and E' are the incoming and outgoing lepton energies, ν is the difference between them, $y = \nu/E$, $x = Q^2/2m_N\nu$, and F_2 (whose Q^2 dependence will generally be tacit) is

$$F_2(x) = \sum e_i^2 x q_i(x), \quad (2)$$

where e_i is the quark charge in units of proton charge and q_i is the distribution function for a quark of flavor i .

B. Backward nucleons from $2N$ correlations

We will speak of observing a backward proton for the sake of definiteness; observing a backward neutron is essentially similar.

Some things change in the above formula when a backward proton is observed. The neutron, which is the struck particle, is not at rest in the laboratory frame. Then the momentum fraction of the struck quark relative to the neutron is not x but rather ξ ,

$$\xi = \frac{x}{2-\alpha}, \quad (3)$$

where $\alpha = (E_p + p^z)/m_N$ is the light-cone momentum fraction of the backward proton with p^z positive for a backward proton. One should also replace $m_N E$ by its corresponding Lorentz invariant,

$$m_N E \rightarrow p_n \cdot k = m_N E(2-\alpha). \quad (4)$$

Also, if we want a backward proton, there is a further factor of the probability density for finding the proton with its observed momentum at the moment the neutron was struck. Thus

$$\begin{aligned} \sigma_{2N} &\equiv \frac{d\sigma_{2N}}{dx dy d\alpha d^2 p_T} \\ &= \frac{4\pi \alpha_{\text{em}}^2 m_N E}{Q^4} \left[1 + (1-y)^2 \right] \\ &\quad \times (2-\alpha) F_2n(\xi) |\psi(\alpha, p_T)|^2, \end{aligned} \quad (5)$$

where p_T is the transverse momentum of the backward proton and we used the light-cone wave function normalized by

$$\int d\alpha d^2 p_T |\psi(\alpha, p_T)|^2 = 1. \quad (6)$$

The neutron structure function F_{2n} is (we shall suppose) known. The test we propose is to measure the cross section for backward nucleon production at a variety of x and α and examine the ratio

$$R_1 = \frac{\sigma_{\text{meas}}/K}{F_{2n}(\xi)}. \quad (7)$$

Here, σ_{meas} is the measured differential cross section and K is the factor

$$K = \frac{4\pi \alpha_{\text{em}}^2 m_N E}{Q^4} \left[1 + (1-y)^2 \right]. \quad (8)$$

The signature of a two-nucleon correlation model is that this ratio is independent of x for any fixed α and p_T . Of course, how useful this signature is depends upon how different we may expect the result to be for a $6q$ cluster. This we shall see in the next section.

C. Backward nucleons from $6q$ clusters

For the case of electromagnetic scattering from the $6q$ state, we have basically the convolution of $F_2^{(6)}$ with the fragmentation functions of the five- (or more, in general) quark residuum. Since the quarks in the residuum depend on which flavor quark was struck, we must write

$$\begin{aligned} \sigma_{6q} &\equiv \frac{d\sigma_{6q}}{dx dy d\alpha d^2 p_T} \\ &= K \sum_i x e_i^2 V_i^{(6)}(x) \frac{1}{2-x} D_{p/5q}(z, p_T). \end{aligned} \quad (9)$$

Here $V_i^{(6)}$ is the distribution function for a valence quark in a six-quark cluster, the sum is over quark flavors, and $D_{p/5q}$ is the fragmentation function for the $5q$ residuum, i.e., the probability density per unit z and p_T for finding a proton coming from the $5q$ cluster. It is tacit that the correct $5q$ cluster, either $u^2 d^3$ or $u^3 d^2$, is chosen. Argument z is the fraction of the residuum's light-cone longitudinal momentum that goes into the proton,

$$z = \frac{\alpha}{2-x}; \quad (10)$$

the factor $(2-x)^{-1}$ comes because $D_{p/5q}$ is probability per unit z in its definition and we quote the differential cross section per unit α . The formula is written for high backward proton momentum, where we can expect the $5q$ residuum and hence the actual $6q$ initial state to dominate.

Neither $F_2^{(6)}$ nor $D_{p/5q}$ can be said to be known. However, since a large fraction of the short-range part of the baryon number two state may be in a six-quark cluster, we should make the best guess as to what these functions might be and see how large a difference it could make experimentally to have significant $6q$ cluster contributions, at least in given regions of phase space.

Estimates of $F_2^{(6)}$ in a model where the nuclei are treated as containing some fraction $6q$ clusters have been

given by Lassila and Sukhatme [10]. They chose their quark distributions beginning with quark-counting rules and then fine-tuned with physical logic to describe the EMC data. For completeness, the three parametrizations they present are recorded in the Appendix.

The fragmentation function is even less well known since there is no complete body of data to check it against. The counting rules suggest a cubic dependence, as (unnormalized)

$$D_{p/q^5}(z) \propto (1-z)^3, \quad (11)$$

for $z \rightarrow 1$ and for zero p_T . We shall use this form, although we keep in mind the possibility that higher order contributions or renormalization group considerations could somewhat alter the power, as they do in many parametrizations of the quark distributions in nucleons.

If the high momentum backward protons come from a six-quark cluster, then $\sigma_{\text{meas}} = \sigma_{6q}$ and the experimental ratio R_1 should be given by

$$R_1 = R_1^{(6)} = \frac{F_2^{(6)}(x) D_{p/5q}(z, p_T)}{(2-x)(2-\alpha) F_{2n}(\xi)}. \quad (12)$$

There is no reason for $R_1^{(6)}$ to be independent of x for fixed α and p_T . We plot this R_1 in Figs. 1 and 2 for $p_T = 0$ and specified α . Some simple quark distributions of Carlson and Havens [11] were used to get F_{2n} in Fig.

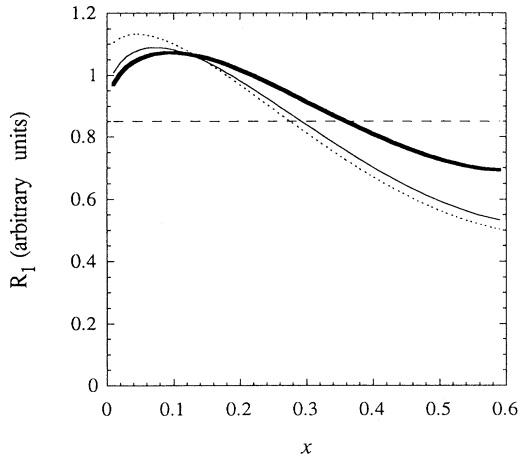


FIG. 1. A putative ratio R_1 assuming the measured cross section for backward protons in deep inelastic scattering is dominated by six-quark configurations and using the LS model [9] for the distribution functions of the six-quark cluster. In general, R_1 is the measured cross section (sans some kinematic factors) divided by the neutron structure function F_{2n} . If backward proton production were dominated by two-nucleon correlations, the plot would be horizontal, like the dashed line. The plot is for fixed $\alpha = 1.4$ (momentum 322 MeV for directly backward protons) and uses CH [10] distribution functions to obtain F_{2n} . The heavy curve is from LS parametrization A, the normal curve is from parametrization B, and the dotted curve is from parametrization C. The vertical units are arbitrary as the fragmentation function $D_{p/5q}$ is not normalized.

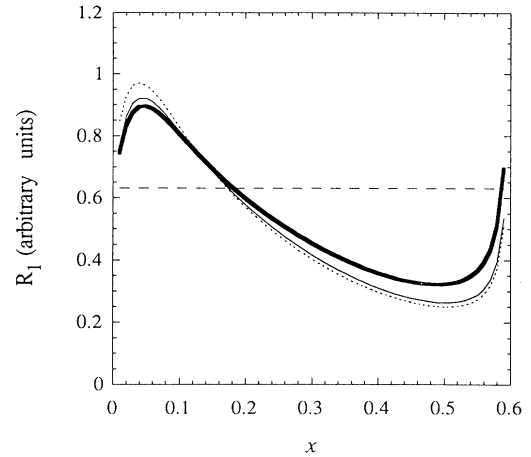


FIG. 2. Like Fig. 1 except that F_{2n} is gotten from the CTEQ [11] distribution functions, specifically from the set CTEQ1L for $Q^2 = 4 \text{ GeV}^2$. The horizontal dashed line is an expectation from $2N$; the other curves are for the $6q$ cluster. The heavy curve is from LS parametrization A, the normal curve is from parametrization B, and the dotted curve is from parametrization C. The curves turn up as $x \rightarrow 0.6$ ($\xi \rightarrow 1$) because the CTEQ distribution functions all approach zero at the upper limit faster than $(1-\xi)^3$, and the fragmentation function we use goes to zero as $(1-z)^3$.

1 and the CTEQ1L [12] distributions were used in Fig. 2. The difference between what is seen and the horizontal line expected from a pure $2N$ correlation model is not negligible. That the ratio goes to a finite value as we reach the kinematic limit $x = 2 - \alpha$ in Fig. 1 has to do with the fact that both the $5q$ fragmentation function and the dominant quarks in the nucleon approach their end points cubically in our models. A dive to zero or a flight to infinity is not precluded in real life, and the latter is seen in Fig. 2.

III. COMMENTS

A. Potential dominance of $6q$ clusters

We expect that a correct description of the deuteron would have a neutron and a proton treated as in the $2N$ model when they are far apart. As they get closer, QCD processes such as gluon recombination [13] will surely occur and affect first the ocean parton distributions. It is something of a simplification to think of a deuteron as just a combination with a large fraction pure $2N$ state with a small fraction (perhaps 5%, from wave function overlap estimates [14]) of the $6q$ state added in.

However, while a $6q$ cluster may be a small part of the deuteron overall, it could be a large fraction of the short-range part of the deuteron wave function. In contrast to the EMC effect, where $6q$ cluster contributions are necessarily diluted by the mostly ordinary collection of nucleons in the target, here we can select events to enhance $6q$ cluster effects. Observing a fast backward proton is a tag that emphasizes the short-range part of

the wave function, and if the $6q$ cluster is there, it could dominate the cross section when the backward proton momentum is large enough. The deviation from what is expected in a pure $2N$ correlation could indeed be as large as shown in our figures.

It is possible and even likely that backward protons will come from some mixture of $2N$ and $6q$ states, with a smooth transition between low backward momentum protons that come mostly from $2N$, to high backward momentum protons that have significant contributions from $6q$. The observed results will move with increasing backward proton momenta from a horizontal line on our figures toward the curves shown for the $6q$ models. How high a backward momentum is needed to get a significant $6q$ contribution? We suggest 300 MeV/ c is a good starting point, based on existing backward proton data from deep inelastic neutrino scattering and studies of the backward proton spectrum in that process using $6q$ cluster ideas.

We do not expect multiple internal scattering to be significant in the deuteron case even in the $2N$ model. In hadron-deuteron elastic scattering it is well known that two 90° scatterings often give a bigger rate than one 180° scattering. In the present case, the scattering that breaks up the struck nucleon is necessarily almost forward, and advantages of multiple scattering do not exist.

B. Possibilities at 4 or 6 GeV electron accelerators

Can an electron accelerator like CEBAF with a 4 or 6 GeV beam be useful? We believe so for the 6 GeV beam. The question centers around how much backward momentum is possible with an incoming electron of this energy, and how much data we can get in the scaling region.

1. Limits on backward proton momentum

The maximum directly backward proton momentum when an electron scatters from a deuteron is $(3/4)m_N$, or 704 MeV, but this is for the case of infinite incoming energy. If the energy is finite, the magnitude of the maximum backward momentum is reduced. For example, with $E = 4$ GeV and $Q^2 = 1$ GeV, the maximum directly backward proton momentum is

$$p^z \leq 0.600m_N = 564 \text{ MeV}, \quad (13)$$

which is still a decent backward momentum. (For a 6 GeV electron beam and the same Q^2 , the maximum p^z is 609 MeV.)

These results were obtained with the help of

$$\alpha m_N \leq \frac{1}{2} \left(m_d + \nu - \sqrt{\nu^2 + Q^2} \right) \times \left\{ 1 + \sqrt{1 - \frac{4m_N^2}{2m_d\nu - Q^2 + m_d^2}} \right\}, \quad (14)$$

and also, for no transverse momentum,

$$p^z = m_N \frac{\alpha^2 - 1}{2\alpha}. \quad (15)$$

For $\nu \rightarrow \infty$, we recover the limits cited, for example, in [3]. Now at finite energy and for a given Q^2 we maximize the limit on p^z by maximizing ν . We have

$$\nu = E - \frac{Q^2}{4E \sin^2(\theta/2)} \leq E - \frac{Q^2}{4E}. \quad (16)$$

For $Q^2 = 1$ GeV² and $E = 4$ GeV, we get $\alpha \leq 1.77$ and p^z as quoted above.

Much of the limitation actually comes because fixing Q^2 for a given incoming energy puts a lower limit on Bjorken x . Since this is also the momentum fraction of the struck quark in the laboratory frame, it means that the struck quark is not moving forward as fast as possible, and the residuum is then not moving backwards as fast as possible. For the 4 GeV beam and the present Q^2 limit, $x_{\min} = 0.14$. If we went to infinite energy, but maintained this value of x , α would still be limited by $\alpha \leq 2 - x_{\min} = 1.86$.

2. Scaling window

Using the formulas with the scaling result for F_{2n} requires that we be in the scaling region. This will squeeze the allowed range of x to be narrower than the kinematic limits.

Scaling requires, at a minimum, that Q^2 be above 1 GeV² and that W (the photon plus single target nucleon c.m. energy) be above 2 GeV, out of the resonance region.

The lower limit on Q^2 sets a lower limit to x , since for a given energy there is a maximum energy transfer ν possible. The maximum ν comes for backward electron scattering and leads to $\nu \leq E - Q^2/4E$ or

$$x_{\min} = \frac{4E Q_{\min}^2}{2m_N (4E^2 - Q_{\min}^2)}. \quad (17)$$

The lower limit on W sets an upper limit on x . Applying the limit to the final state that comes from striking the neutron in the $2N$ correlation model gives

$$W^2 = (p_n + q)^2 = m_N^2 + 2m_N \nu (2 - \alpha) - Q^2 \geq W_{\min}^2, \quad (18)$$

for a given α of the backward proton and letting $p_n^2 = m_N^2$. This leads to a limit, also reached for 180° scattering, that

$$x_{\max} = \frac{2E [2m_N E (2 - \alpha) - (W_{\min}^2 - m_N^2)]}{m_N [4E^2 + (W_{\min}^2 - m_N^2)]}. \quad (19)$$

The curves giving x_{\max} and x_{\min} are shown in Fig. 3 for $\alpha = 1.4$. The scaling region is the region between the two curves.

For $\alpha = 1.4$, the scaling region includes only a short span of x for electron energy $E = 4$ GeV, but the span increases greatly for $E = 6$ or 8 GeV. The span for 8 GeV is over half of the maximum possible at any energy, and not too much less than could be got at 15 GeV. For increasing α , which corresponds to increasing velocity of the struck neutron away from the photon, larger energy in the laboratory is needed to reach the scaling region.

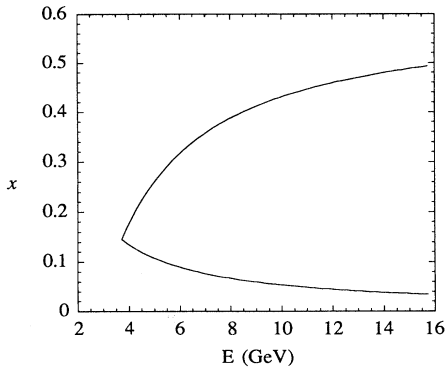


FIG. 3. The scaling window for $\alpha = 1.4$. Values of x between the two curves can be reached in the scaling region for a given incoming electron energy E , given in GeV above. The lower curve is set by the requirement that $Q^2 \geq 1 \text{ GeV}^2$ and the upper curve by the requirement that $W \geq 2 \text{ GeV}$. The curves begin at $E = 3.72 \text{ GeV}$ for this α .

3. Outside the scaling region

Do we need to be in the scaling region? Our formulas for the $2N$ correlation are simplest to evaluate there, and we do not know how to guess at forms for production off the $6q$ component; so our comparison case is gone. But from the $2N$ viewpoint, the purpose of scattering off the neutron is to free the proton—nothing more. If all we want is a yes or no on the $2N$ correlation model, we could take a measured cross section for producing backward protons and divide by a cross section for scattering off a neutron at the correct values of the incoming variables, and see if the result depends only upon α and p_T .

The disadvantage of doing this may be more practical. Driving the struck particles forward forcefully separates them greatly in momentum space from the backward proton and reduces the final state interactions, which we have neglected in our discussion. As we leave the scaling region, it can mean that the energy transferred to the forward moving particles is low enough that we need to rethink our attitude towards final state interactions.

C. Possibilities with electrons or muons at higher energy

There is a number of existing or proposed accelerators or facilities—for example, ELFE, Hermes at DESY, HELP at LEP, or Fermilab—that can observe backward nucleons from electron or muon scattering from fixed targets. There is a clear advantage in not having to think about the “scaling window.” It is virtually the full possible kinematic range.

At Fermilab, to take one case, experiment E665 scattered 490 GeV muons from deuterium and xenon targets in a streamer chamber so as to be able to observe backward charges. A later version of experiment E665 has capability to observe backward neutrons, and uses carbon, calcium, and lead as its heavier targets. There is some rate advantage in measuring backward neutrons instead

of protons. For the $6q$ model, if the valence configuration dominates, as it should at high backward nucleon momenta, then the ratio of neutron rate to proton rate should be $3/2$ and be independent of x . (One uses a combinatoric argument to get ratios of proton and neutron production from u^3d^2 and u^2d^3 residua, and some discussion of this appears in [4].) The result for the $2N$ model is different, since one has

$$\frac{\sigma_{2N}(\mu d \rightarrow \mu n X)}{\sigma_{2N}(\mu d \rightarrow \mu p X)} = \frac{F_{2p}(\xi)}{F_{2n}(\xi)}, \quad (20)$$

so that the ratio should vary from about 1 at low ξ to about 4 at high ξ . Thus backward neutrons are always produced more copiously, and there is an interesting comparison of observables if one has the capability of detecting both flavors of nucleons.

We might also note that study of backward nucleons from a deuteron target is a study of the “target fragmentation region” and is best and most easily carried out in the rest frame of the target, i.e., the laboratory. Data presented in the photon-target c.m. are not equally useful.

D. Falling $\langle x \rangle$ with increasing α

Let us point out a piece of kinematics. From momentum conservation one has $0 \leq x \leq (2 - \alpha)$. Hence, unless the x distribution has a bizarre shape, one expects that $\langle x \rangle_\alpha$ —the average value of x at fixed α —decreases as α increases. This was pointed out in Ref. [2] in the context of the $2N$ model, and was initially suggested as a test of that model. However, the result should be produced by any model, and so finding the trend in the data is not startling.

The two-nucleon correlation model does give a specific result that $\langle x \rangle_\alpha$ falls to zero linearly as $2 - \alpha$. In contrast, the six-quark cluster model may or may not fall quite linearly. It depends on the specific implementation of the model.

The rest of this subsection attempts to show why the two-nucleon result for $\langle x \rangle_\alpha$ is independent of the internal details of that model, but similar manipulations for other models do not lead to such definite results. It has to do with the way the cross section factors.

For the two-nucleon model, the structure of the formula for the cross section differential in x and α is

$$P(x, \alpha) = \frac{dN}{dx d\alpha} = f(\xi) \frac{|\psi(\alpha)|^2}{2 - \alpha}, \quad (21)$$

where ξ is defined earlier. An elementary calculation gives

$$\langle x \rangle_\alpha = \frac{\int_0^{2-\alpha} dx x P(x, \alpha)}{\int_0^{2-\alpha} dx P(x, \alpha)} = (2 - \alpha) \langle \xi \rangle, \quad (22)$$

where $\langle \xi \rangle$ is independent of α . We can easily turn this into

$$\frac{\langle x \rangle_\alpha}{\langle x \rangle_{\alpha=1}} = (2 - \alpha). \quad (23)$$

The sort of result that can be derived in the corre-

sponding way for the six-quark cluster appears less useful. We envision one quark being struck and driven forward, and the residuum that remains “fragments” (or recombines) into a nucleon, which often goes backward, plus other stuff. The differential cross section is structurally

$$P(x, \alpha) = \frac{dN}{dx d\alpha} = \frac{g(x)}{2-x} D\left(z = \frac{\alpha}{2-x}\right). \quad (24)$$

The factor $g(x)$ is for the quark knockout and $D(z)$ is the fragmentation function. The first is a function of x since it involves distribution functions of quarks in the six-quark cluster, and the six-quark cluster is standing still in the laboratory. Argument z is defined earlier. The neatly derivable result is for average α at fixed x :

$$\langle \alpha \rangle_x = \frac{\int_0^{2-x} d\alpha \alpha P(x, \alpha)}{\int_0^{2-x} d\alpha P(x, \alpha)} = (2-x)\langle z \rangle \quad (25)$$

or

$$\frac{\langle \alpha \rangle_x}{\langle \alpha \rangle_{x=1}} = (2-x). \quad (26)$$

This result for the six-quark cluster contribution requires averaging over all α , and while the optimist may expect the six-quark contributions to dominate at high α , no one expects them to do so at moderate α . So this result seems untestable.

For $\langle x \rangle_\alpha$ details would have to be worked out for each special case. However, remembering the general result that $\langle x \rangle_\alpha$ decreases with increasing α and is zero kinematically when $\alpha = 2$ makes it likely that one will get something like the $2N$ result.

IV. CONCLUSION

Study of the deuteron should be pursued since deuterons are our chief source of information about neutrons and we should understand this source. Further, the behavior of the deuteron state at short range gives information about the short-range dynamics of strong interaction QCD.

We have suggested a measurement to learn what the short-range wave function of the deuteron is. Namely, examine the shape of the measured differential cross section for electroproduction of backward protons or neutrons from a deuteron target, and take its ratio to what would be expected for deep inelastic scattering from a

free neutron or proton, respectively. A high momentum backward nucleon acts as a tag isolating events where the initial material in the deuteron was tightly bunched. The x dependence or lack of x dependence of the ratio is a signal that is distinct for the extreme cases of a pure $2N$ or pure $6q$ cluster. We have presented simple model estimates of the size of effects that may be seen, showing that factors of 2 differences from maximum to minimum may be expected in the $6q$ case, whereas no maximum to minimum difference is expected in the $2N$ case.

ACKNOWLEDGMENTS

C.E.C. thanks the National Science Foundation for support under Grant No. PHY-9112173 and K.E.L. thanks the Department of Energy for support under DOE Grant No. W-7405-ENG-82 Office of Energy Research (KA-01-01). We also thank Keith Griffioen, Jorge Morfin, Brian Quinn, and Mark Strikman for useful remarks.

APPENDIX: DISTRIBUTIONS FOR SIX-QUARK CLUSTERS

We apply the notation $|6q\rangle$ or $6q$ to label the situation when the neutron and proton are melded and lose their individual identity. This notation emphasizes the fact that standard QCD quark parton model considerations should be applied to this interesting multi-quark object. Therefore, for a generic $|nq\rangle$ state the sea, valence, and gluon distribution functions (times z) are written

$$\begin{aligned} \bar{U}_n(z) &= A_n(1-z)^{a_n}, \\ V_n(z) &= B_n z^{1/2}(1-z)^{b_n}, \\ G_n(z) &= C_n(1-z)^{c_n}, \end{aligned} \quad (A1)$$

where z is the fraction of the total cluster momentum. The coefficients and powers are determined in [10] by appealing to standard normalization and momentum conservation considerations along with input information from experimental study of the $n = 2$ (pion) and $n = 3$ (nucleon) situations. As a result, three cases were developed to illustrate the sensitivity to small changes in the power of $(1-z)$, i.e., $(a_6, b_6) = (11, 9)$ for case A, $(11, 10)$ for case B, and $(13, 10)$ for case C. For completeness we give $(A_6, B_6) = (1.429, 1.762)$ for case A, $(1.478, 1.850)$ for case B, and $(1.725, 1.850)$ for case C.

-
- [1] V. Matveev and P. Sorba, *Nuovo Cimento A* **45**, 257 (1978); A.P. Kobushikin (Kobushikin in newer works by the same author), *Yad. Fiz.* **28**, 495 (1978) [*Sov. J. Nucl. Phys.* **28**, 252 (1978)]; P. González and V. Vento, *Few-Body Syst.* **2**, 145 (1987).
- [2] L.L. Frankfurt and M.I. Strikman, *Phys. Lett.* **69B**, 93 (1977).
- [3] C.E. Carlson, K.E. Lassila, and U.P. Sukhatme, *Phys. Lett. B* **263**, 277 (1991).
- [4] C.E. Carlson and K.E. Lassila, *Phys. Lett. B* **317**, 205 (1993).
- [5] E. Matsinos *et al.*, *Z. Phys. C* **44**, 79 (1989).
- [6] V.V. Ammosov *et al.*, *Sov. J. Nucl. Phys.* **43**, 759 (1986).
- [7] V.I. Efremenko *et al.*, *Phys. Rev. D* **22**, 2581 (1980).
- [8] J.P. Berge *et al.*, *Phys. Rev. D* **18**, 1367 (1978).
- [9] C. Ciofi degli Atti, S. Simula, L.L. Frankfurt, and M.I. Strikman, *Phys. Rev. C* **44**, R7 (1991).
- [10] K.E. Lassila and U.P. Sukhatme, *Phys. Lett. B* **209**, 343

- (1988).
- [11] C.E. Carlson and T.J. Havens, Phys. Rev. Lett. **51**, 261 (1983).
- [12] J. Botts *et al.*, Phys. Lett. B **304**, 159 (1993).
- [13] A. Mueller and J.W. Qiu, Nucl. Phys. **B268**, 427 (1986);
- F. Close, R. Roberts, and J.W. Qiu, Phys. Rev. D **40**, 2820 (1989).
- [14] M. Sato, S. Coon, H. Pirner, and J. Vary, Phys. Rev. C **33**, 1062 (1986).